LEP 200 PHYSICS

J. MNICH
RWTH Aachen, III. Phys. Inst. B, Aachen, D-52056, Germany
E-mail: Joachim.Mnich@Physik.RWTH-Aachen.de

This article summarises recent results obtained by the four experiments ALEPH, DELPHI, L3 and OPAL at the LEP e^+e^- collider at centre-of-mass energies up to $\sqrt{s} = 202$ GeV. The experimental results discussed here comprise the production of fermion pairs, of neutral and charged bosons together with studies of their properties. All measurements are compared to the expectations of the Standard Model of electroweak interactions. The measurement of the mass of the W boson is combined with other precision measurements of electroweak observables which provides an estimate of the mass of the last undiscovered particle of the Standard Model, the Higgs boson. The article is complemented by a discussion of the direct searches for Higgs bosons and Supersymmetric particles at these highest energies attained so far in e^+e^- collisions.

1 Introduction

The Large Electron-Positron Collider (LEP) at CERN in Geneva started in 1989 to operate at centre-of-mass (cms) energies close to the mass of the Z boson. This first phase (LEP I) has been concluded in 1995. The four experiments collected a total of about 16 million decays of the Z into hadrons and leptons. This large data sample allows the very precise measurement of Z parameters and tests of the Standard Model [1] (SM) beyond the tree level. Many other physics results have been obtained, and are still obtained, from careful analyses of these data. Examples are tests of Quantum Chromodynamics (QCD) as well as the physics of the b-quark and the tau lepton.

In the autumn of 1995 the LEP machine began to raise in steps the cms energy beyond the Z resonance. This has been possible after installation of additional super-conducting radio frequency cavities required by the larger energy loss due to synchrotron radiation at higher beam energies. This second phase (LEP II) is marked by operating at energies above the W pair production threshold. The performance of the collider was steadily increased leading to higher luminosities and energies up to a maximum of $\sqrt{s} = 202$ GeV attained in 1999. Table 1 summarises the operation of LEP from the end of 1995 to 1999.

At LEP II the experiments are performing measurements of the W-pair cross section $e^+e^- \to W^+W^-(\gamma)$ as function of the cms energy, the determination of the W mass and the study of triple gauge boson couplings. In addition, the increase in energy allows the exploration of new kinematic regions in the

Table 1. Summary of the LEP operation above the Z resonance. Listed are the approximate cms energies and the integrated luminosities collected on average by each experiment.

Year	$\sqrt{s}$	$\int \mathcal{L}\,\mathrm{d}t$
1995	$130-140$ GeV	5 pb^{-1}
1996	161/172 GeV	21 pb^{-1}
1997	183 GeV	55 pb^{-1}
	130/136 GeV	7 pb^{-1}
1998	189 GeV	180 pb^{-1}
1999	$192-202$ GeV	240 pb^{-1}

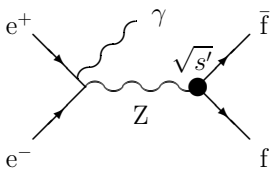

Figure 1. Fermion-pair production with initial state photon radiation.

search for new particles, in particular for the SM Higgs boson [2] and Supersymmetric [3] (SUSY) particles. Other important fields investigated at LEP II are studies of fermion-pair production, tests of QCD and two-photon physics.

In this article some selected results are presented with emphasis on tests of the SM and searches for Higgs bosons and SUSY particles. Many of these results are still preliminary and all limits are set at 95% confidence level (CL).

2 Fermion-Pair Production above the Z Resonance

In the energy range of LEP II, well above the Z resonance, the total cross sections for $e^+e^- \to f\bar{f}$ are about two orders of magnitude smaller than at the Z pole. Initial state radiation (Figure 1) plays an important role. Radiation of one or more photons by the incoming electrons removes energy from the annihilation process and the fermion production takes place at a lower effective cms energy, $\sqrt{s'}$, where the cross section is different. In particular, if the remaining energy in the e^+e^- system is close to the mass of the Z the annihilation cross section is very high. Consequently this provides a major contribution to the total cross section $e^+e^- \to f\bar{f}$ and it is called radiative 'return-to-the-Z'. If the initial state photon is detected its measured energy can be used to calculate $\sqrt{s'}$. However, in general photons are emitted at small

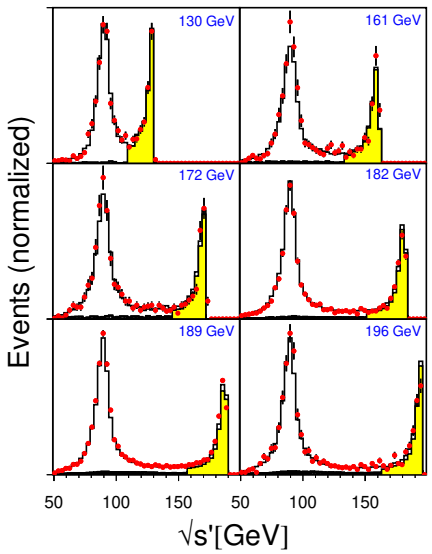

Figure 2. Distribution of the reconstructed effective cms energy, $\sqrt{s'}$, in the reaction $e^+e^- \rightarrow$ hadrons(γ) at various cms energies above the Z resonance. The dots are L3 data and the histograms are obtained from Monte Carlo simulations. The shaded areas correspond to $\sqrt{s'/s} > 0.85$.

angles by the incoming electron or positron and thus often escape detection through the beam pipe. In this case the photon energy can be determined from the polar angles of the outgoing fermions.

The importance of the return-to-the-Z is illustrated in Figure 2 which shows the distribution of the effective cms energy at various LEP energies above the Z pole. In addition to the peak at the nominal cms energy, with a smooth tail towards lower energies from the radiation of soft photons, one observes that a large fraction of the events is actually produced at $\sqrt{s'} \approx m_{\mathrm{Z}}$.

Because of the different nature of events produced at, or close to, the nominal cms energy and those stemming from decays of real Z bosons the LEP experiments measure two sets of cross sections and forward-backward asymmetries: for the total sample and the high energy events separated by a cut in the reconstructed $\sqrt{s'}$ value.

Results of the total cross section measurements for hadrons and muon pairs above the Z pole from the OPAL experiment are shown in Figure 3 for both the total event sample and the high energy events alone. The measure-

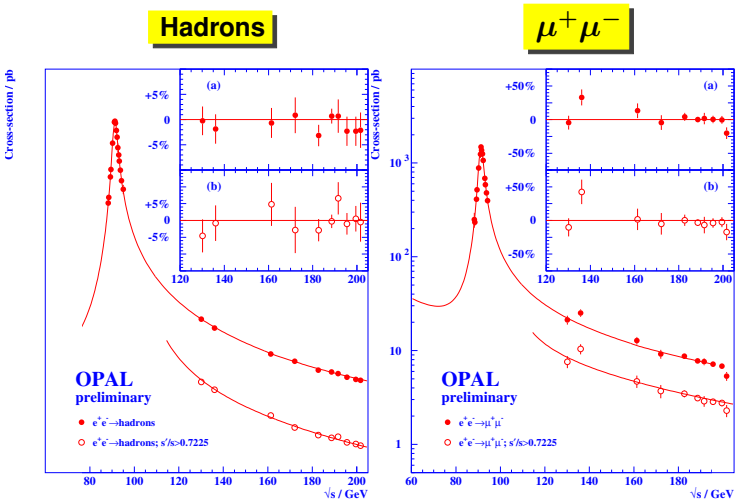

Figure 3. Measurements of the total cross sections $e^+e^- \to$ hadrons and $e^+e^- \to \mu^+\mu^-$ by the OPAL experiment from the Z pole to 202 GeV. The inlets show the ratios of the measurements and the SM expectations.

ments are compared to the SM expectations as calculated with the programs ZFITTER [4] and, for $e^+e^- \to e^+e^-(\gamma)$, TOPAZ0 [5]. Similarly, the results on the forward-backward asymmetry of charged leptons are shown in Figure 4. Good agreement is observed between the measurement and the SM prediction. Results and details on the analyses can be found in References [6,7,8,9].

An analysis which profits from the presence of the radiative return-to-the-Z is the study of the reaction $e^+e^- \to \nu\bar{\nu}\gamma$. This process gives rise to high energy single photons in the detector. At $\sqrt{s} = 189$ GeV about 500 such events are observed by each experiment and Figure 5 shows an example of the measured photon energy spectrum [10].

The cross section, for photons within the polar angular range $\cos\theta_\gamma \leq 0.97$ and with $E_\gamma \geq 5$ GeV, as a function of the cms energy is also shown in Figure 5. From this measurement the number of light neutrino families can be derived. A combination of LEP results above the Z pole yields $N_\nu = 2.99 \pm 0.10$, in agreement with the more accurate determination from the difference of the measured total and visible decay widths of the Z boson, $N_\nu = 2.9835 \pm 0.0083$ [11,12].

Employing techniques similar to those used at the Z resonance, b- and c-quarks are identified in hadronic events allowing the measurements of cross

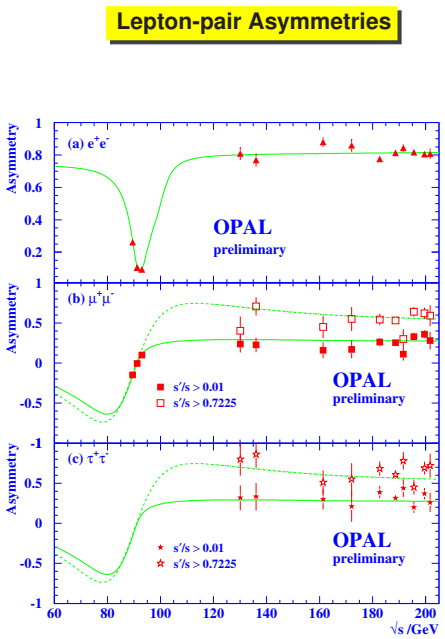

Figure 4. Measurements of the forward-backward asymmetry in pair production of electrons, muons and taus by the OPAL experiment.

sections and forward-backward asymmetries [6,13,14,15]. Cross section measurements are expressed in terms of R_{q} ($\mathrm{q} = \mathrm{b}, \mathrm{c}$) which above the Z resonance is defined as ratio of individual quark cross sections to the sum of the five flavours produced at LEP. Only events with high effective cms energy are considered in these analyses. The measurements of R_{b} and the forward-backward asymmetry by OPAL as function of the cms energy are shown in Figure 6.

All measurements of total cross sections and forward-backward asymmetries of fermion pairs at LEP are in agreement with the SM. This observation allows to put constraints on new physics. A general framework for the description of new phenomena are four-fermion contact interactions [16]. Lower limits on the energy scale of such contact interactions, to be considered as the mass scale of exchanged virtual particles, are set by the experiments in the order of 2 TeV $-$ 10 TeV, depending on the model and the final state. Figure 7 presents the result of the OPAL experiment obtained from inclusive hadron

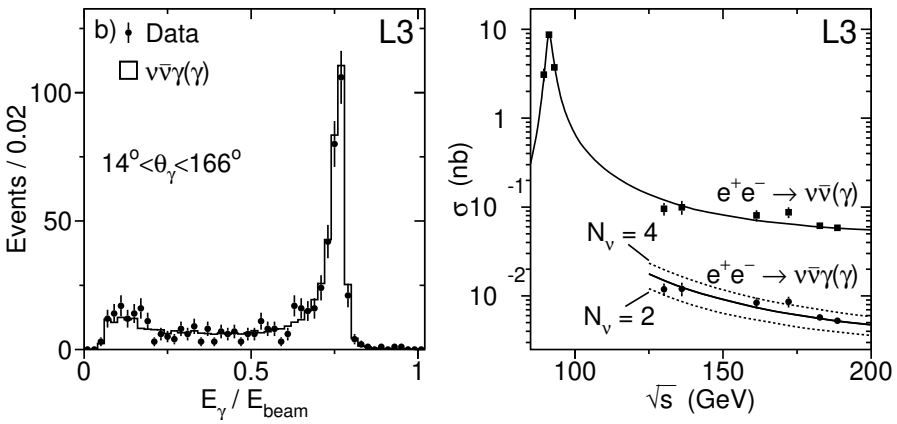

Figure 5. Left: Energy spectrum of single photon events observed by L3 at $\sqrt{s} = 189$ GeV compared to the Monte Carlo expectation. Right: Cross section measurement $e^+e^- \to \nu\bar{\nu}\gamma$ ($E_\gamma \geq 5$ GeV, $\cos\theta_\gamma \leq 0.97$) from the Z resonance to $\sqrt{s} = 189$ GeV compared to the expectations for 2, 3 and 4 neutrino species. The upper curve shows the extrapolated, full cross section $e^+e^- \to \nu\bar{\nu}$.

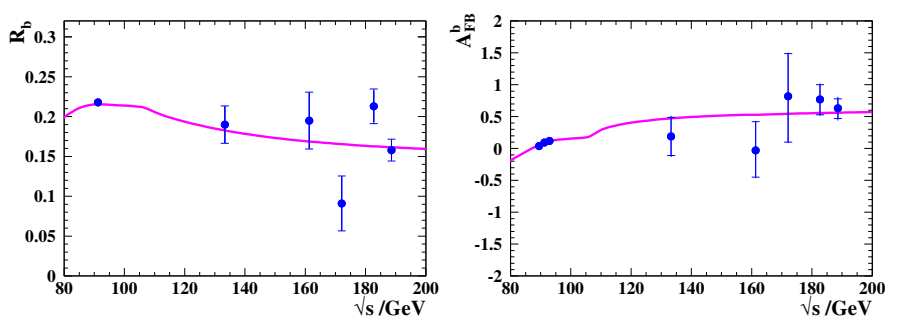

Figure 6. Measurements of R_b (left) and the b-quark forward-backward asymmetry A_FB^b (right) above the Z resonance by OPAL compared to the SM.

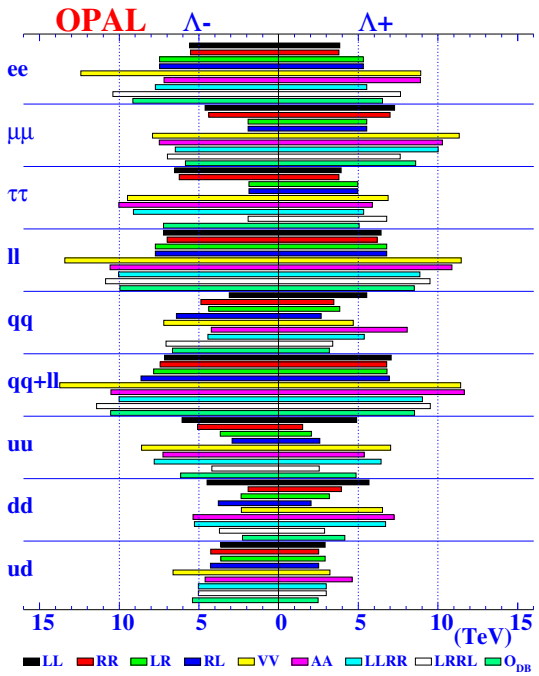

Figure 7. Limits on the energy scale for contact interactions in different scenarios as obtained by OPAL from the measurements of hadronic and leptonic cross sections and forward-backward asymmetries.

and charged lepton final states.

A more specific example for the presence of new physics would be the existence of an additional neutral heavy gauge boson, Z′. Even at cms energies well below its mass the Z′ could modify observables through the interference with the photon and the Z boson. Models resulting from E_6 or left-right symmetries [17] are investigated at LEP resulting in lower limits on the mass as a function of the mixing angle between the Z and the Z′, $\theta_{\rm M}$ (Figure 8). Whereas the precision measurements at the Z pole exclude large mixing angles, the data at higher energies allow to increase the lower mass limit for any $\theta_{\rm M}$. A hypothetical Z′ boson with SM couplings to fermions must have a mass $m_{Z'} > 950$ GeV.

The hadronic events recorded during the runs at $130 \leq \sqrt{s} \leq 189$ GeV are

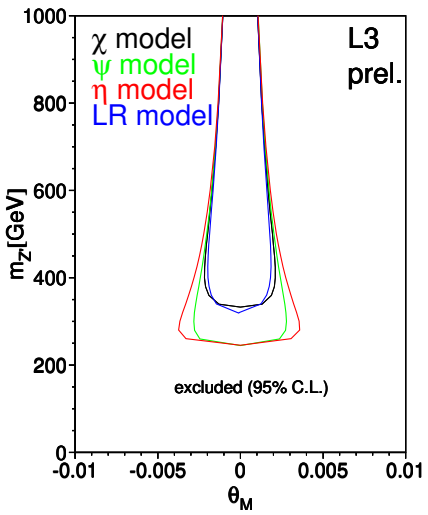

Figure 8. Exclusion limits from L3 on the mass of an additional heavy neutral gauge boson Z' and the $Z - Z'$ mixing angle θ_M in various models.

used to perform studies on the energy evolution of observables and to compare them to the predictions based on QCD. Figure 9 compares the thrust distribution measured by the L3 experiment at $\sqrt{s} = 189$ GeV with various QCD based Monte Carlo models. Good agreement is observed and this thrust distribution, together with other event shape variables, is used to determine the strong coupling constant to be $\alpha_s(189\ \text{GeV}) = 0.1105 \pm 0.0018 \pm 0.0058$ where the first error is experimental and the second reflects theoretical uncertainties [18].

The large range of cms energies explored by the LEP experiments allows the measurement of the strong coupling constant α_s as function of energy. The running of α_s is clearly demonstrated in Figure 9. The same event shape variables are used to determine α_s at the various energies such that theoretical uncertainties do not affect the measured energy dependence.

3 Production of Neutral Bosons

Tests of Quantum Electrodynamics (QED) at the highest energies are possible at LEP by studying photon-pair production $e^+e^- \to \gamma\gamma$. Measurements of total and differential cross sections are performed [19,20,21,22] and good agreement

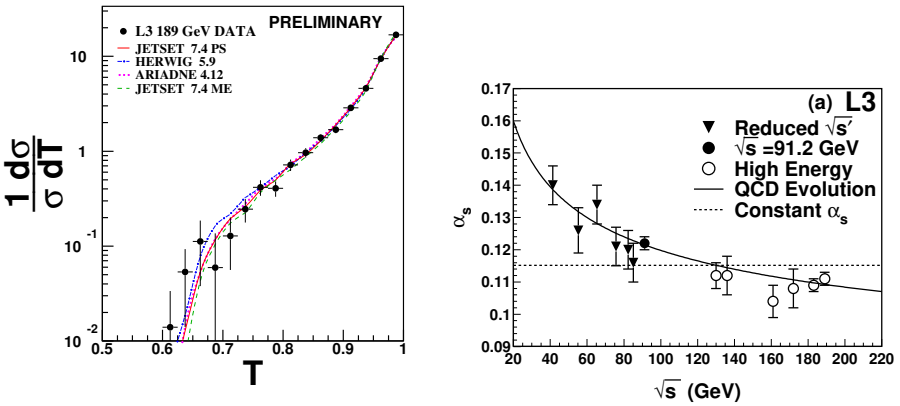

Figure 9. Left: The distribution of thrust in $e^+e^- \to$ hadrons events at $\sqrt{s} = 189$ GeV as measured by the L3 experiment compared to Monte Carlo simulations. Right: The evolution with energy of the strong coupling constant α_s as measured with the same set of hadronic event shape variables in $e^+e^- \to$ hadrons.

with the QED prediction is found up to the highest cms energy. Figure 10 shows as an example the total cross section measured by L3 from the Z resonance up to $\sqrt{s} = 196$ GeV. From these analyses the experiments set lower limits on the QED cut-off parameters $\Lambda_\pm$ and on the mass of an excited electron of the order of 300 GeV.

Another pure QED process studied at LEP is the Compton scattering of quasi-real photons with electrons, $e^\pm\gamma \to e^\pm\gamma$, sketched in Figure 11 [23]. The low virtuality of the initial state photon is ensured by imposing a cut on the reconstructed transverse momentum of the electron it was radiated off. Approximately 6000 events are observed in the data collected between the Z resonance and 189 GeV by the L3 experiment. The cross section of this process as a function of the energy in the system of the scattering electron and photon is measured as shown in Figure 12. Good agreement up to an energy of 160 GeV in the electron-photon system is observed which constrains the mass and coupling of an excited electron.

A similar process, electroweak Compton scattering, where the scattering of the photon results in the production of a Z boson or a highly virtual photon, $e^\pm\gamma \to e^\pm Z/\gamma^*$, is studied by the OPAL collaboration [24]. The decays of the Z or the γ^* into hadrons are investigated and the invariant mass distribution

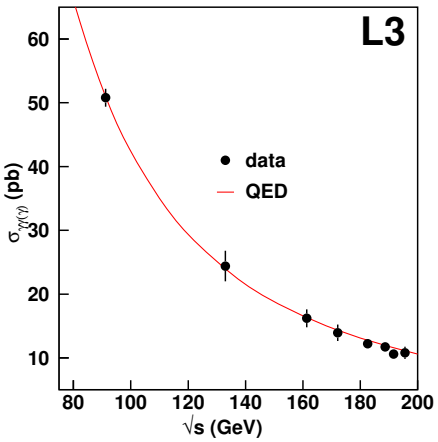

Figure 10. Measurements of the cross section $e^+e^- \to \gamma\gamma$ by L3 between the Z resonance and $\sqrt{s} = 196$ GeV. The solid curve is the SM expectation.

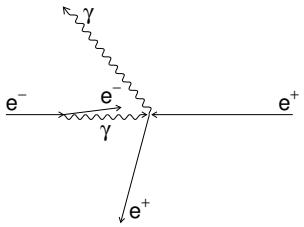

Figure 11. Sketch of Compton scattering of quasi-real photons with electrons at LEP.

of the jet pairs as shown in Figure 12 is observed. The shape and absolute rate measured in the data is in agreement with the expectation allowing a clear distinction between virtual photons, $m_{jj} < 60$ GeV, and the single Z production.

With the cms energy increased to 183 GeV in 1997, LEP attained the threshold for Z-pair production, $e^+e^- \to ZZ$. In the SM this process is mediated by t- and u-channel exchange of an electron with two Feynman diagrams contributing in lowest order (Figure 13). Candidate events are selected as four-fermion final states requiring that the reconstructed invariant masses of

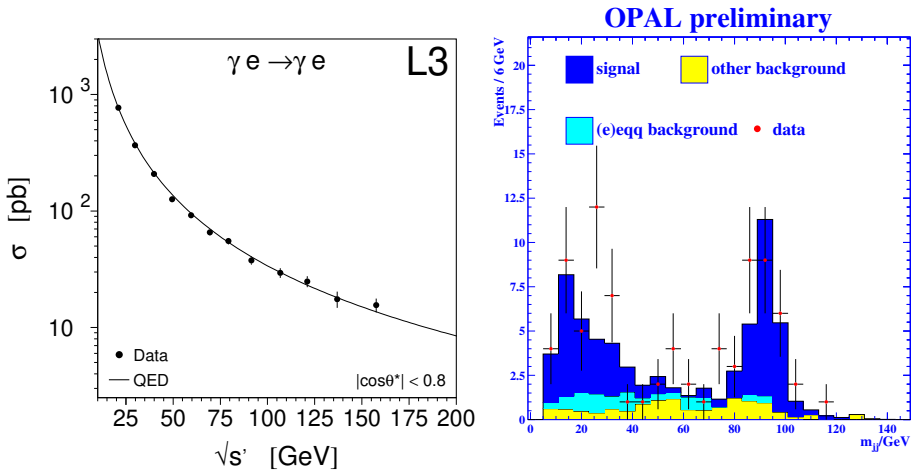

Figure 12. Left: Measured Compton scattering cross section $e\gamma \to e\gamma$ as function of the energy in the electron-photon system, $\sqrt{s'}$. Data taken at cms energies from the Z resonance up to $\sqrt{s} = 189$ GeV are used. Right: Distribution of the jet-pair mass in $e^{\pm}\gamma \to e^{\pm}\,Z/\gamma^*$ candidates observed by OPAL.

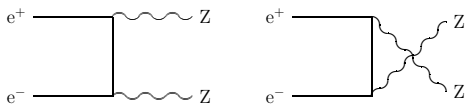

Figure 13. Feynman diagrams contributing to $e^+e^- \to ZZ$ at lowest order.

jet and lepton pairs are consistent with the production of on-shell Z bosons. The sum of the two invariant masses in candidate events of DELPHI collected at $\sqrt{s} = 189$ GeV is displayed in Figure 14. The presence of a $e^+e^- \to ZZ$ signal is clearly visible in the data. This figure also shows the combined LEP cross section measurement as a function of the cms energy which confirms the SM expectation.

4 Production of W Boson Pairs

Since the threshold for W-pair production was attained in 1996 the LEP experiments study the reaction $e^+e^- \to W^+W^-$. The main goals are the

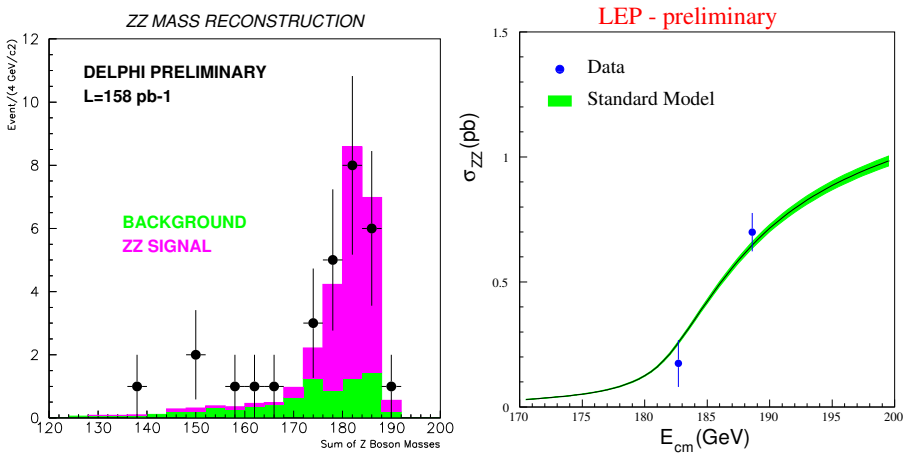

Figure 14. Left: Distribution of the sum of the two reconstructed invariant masses in $e^+e^- \to ZZ$ candidates of DELPHI. Right: Combined LEP cross section measurements of $e^+e^- \to ZZ$ at two cms energies compared to the SM expectation. The shaded band indicates the uncertainty of the SM calculation.

measurement of the cross section as a function of the energy which, together with the measurement of differential cross sections, allows to study the couplings at the triple boson vertices, and the precise measurement of the W mass. Details on the analyses and published results on W physics at LEP can be found in References [29,30,31,32].

Experimentally, three different topologies are distinguished in the production of W-pairs: purely leptonic $e^+e^- \to \ell\nu\ell\nu$ (ℓ = e, μ, τ), which contribute to about 11%, semi-leptonic $e^+e^- \to q\bar{q}\ell\nu$ (44%) and fully hadronic final states $e^+e^- \to q\bar{q}q\bar{q}$ (46%). Contributions to these four-fermion final states from other processes, not involving two on-shell W bosons, have to be calculated from Monte Carlo simulations. Examples are single W production $e^+e^- \to We\nu$ and the exchange of two neutral bosons. Most difficult is the separation of the $e^+e^- \to q\bar{q}q\bar{q}$ signal from QCD four-jet events.

From the cross sections measured individually for the different final states the branching fractions of the W boson into hadrons and the three lepton species are derived (Table 2) [33]. The decay rates into electrons, muons and taus are found to be equal and thus confirming lepton universality in charged current interactions. The hadronic branching ratio depends on the six elements of the Cabbibo-Kobayashi-Maskawa [34,35] matrix not involving the top

Table 2. Combined LEP results on the branching ratios of the W boson into hadrons, the three lepton families and the average leptonic branching fraction.

W →	Measured [%]	SM [%]
hadrons	67.96 ± 0.41	67.5
$e\nu$	10.61 ± 0.25	
$\mu\nu$	10.65 ± 0.24	
$\tau\nu$	10.82 ± 0.32	
$\ell\nu$	10.68 ± 0.13	10.8

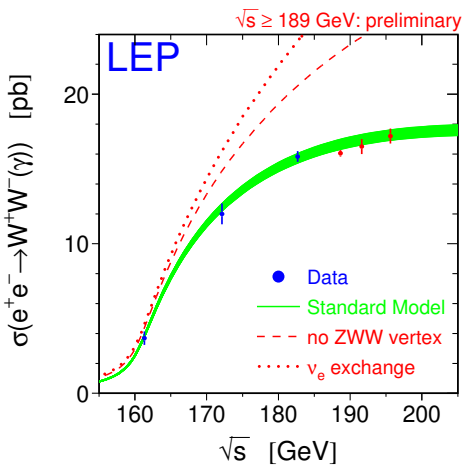

Figure 15. The cross section $e^+e^- \to W^+W^-$ as a function of the cms energy. The combined LEP measurements are compared to the SM prediction shown as a band including the theoretical uncertainty and to hypotheses without triple gauge boson couplings.

quark [36]. By fixing five of them to the world averages [12] the least precise of the two diagonal elements is derived to be $|V_{cs}| = 0.997 \pm 0.020$.

To date about 7000 $e^+e^- \to W^+W^-$ events have been collected by each of the four collaborations at cms energies up to $\sqrt{s} = 202$ GeV. The average cross sections measured by the LEP experiments at cms energy values between the threshold and 196 GeV are shown in Figure 15 [11]. The measurements follow the SM expectation and prove the existence of triple gauge boson couplings. Hypotheses with no ZWW vertex or only t-channel exchange of electron neutrinos are ruled out.

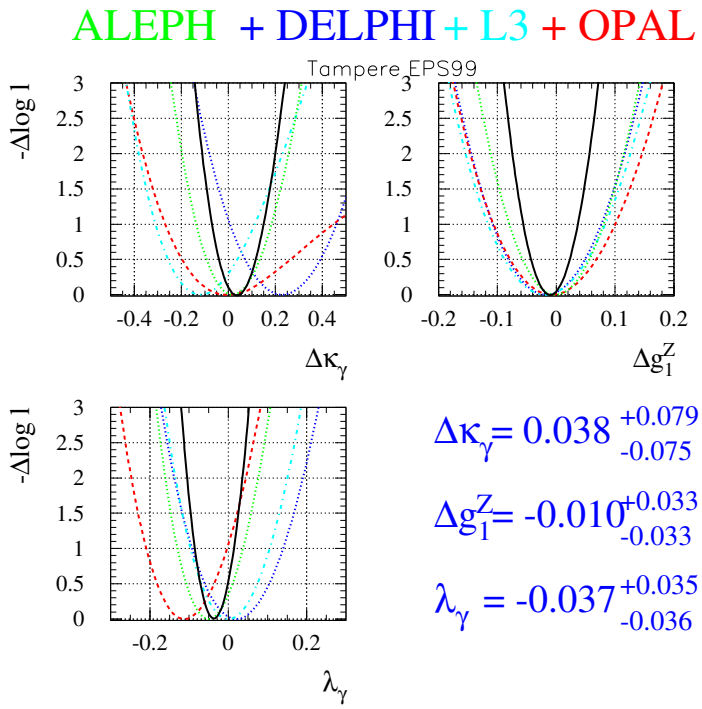

Figure 16. Likelihood curves obtained from the fit for W coupling parameters $\Delta\kappa_\gamma = \kappa_\gamma - 1$, $\Delta g_1^Z = g_1^Z - 1$ and λ_γ by the four experiments and the combined results (solid lines). The central values and errors of the combined result are listed in the right bottom corner.

More information on the couplings of the W boson is contained in the differential distributions of the W production angle and the decay angles in the W rest frame. The couplings of the W boson to the photon and the Z are therefore derived from combined fits to differential and total cross sections.

In the most general Lorentz invariant ansatz the γWW and ZWW vertices are parametrized by 2×7 complex couplings [37]. Because these are too many parameters to be measured simultaneously, real couplings as well as C, P and CP invariance are assumed. Imposing also $SU(2)$ symmetry three coupling parameters remain to be studied [38]. These parameters and their SM model values are:

$$g_1^Z = 1\,, \qquad \kappa_\gamma = 1\,, \qquad \lambda_\gamma = 0\,. \tag{1}$$

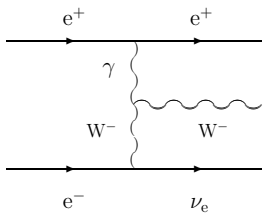

Figure 17. Feynman diagram of single W boson production in e^+e^- collisions.

Deviations from the SM values, denoted by Δ, do not affect the gauge boson propagators at tree level which would lead to observable effects at the Z resonance. The parameter g_1^Z describes the ZWW coupling and the other two are related to the static magnetic dipole and electric quadrupole moment of the W boson.[a]

The results for these coupling parameter obtained in likelihood fits leaving one parameter free at a time while fixing the others to their SM values are shown in Figure 16. Deviation from the SM values are denoted by Δ. All parameters are found to be consistent with their expected values and the current experimental precision is at the percent level.

Additional information on triple gauge boson couplings is contained in the production of single W bosons. This process, sketched in Figure 17, is particularly sensitive to the parameter κ_γ. As this is a t-channel reaction, the final state electron typically escapes along the beam pipe producing spectacular two-jet or single-lepton events with missing energy. The small cross section is measured by the LEP experiments [39,40] and found to be in agreement with the SM. For example the cross section as a function of the cms energy measured by L3 is shown in Figure 18.

Also single photon final states contain information on the WWγ vertex as can be seen from Figure 17 interchanging the role of the W and the photon. The improved determination of κ_γ by ALEPH exploiting all three final states is presented in Figure 18. The result is consistent with the SM: $\Delta\kappa_\gamma = -0.01\,^{+0.14}_{-0.11}$.

In the SM also quartic couplings among the gauge bosons exist. At LEP the vertices WW$\gamma\gamma$ and WWZγ can be studied in the reaction $e^+e^- \to W^+W^-\gamma$. However, their existence cannot be proven because at LEP energies the effect of the SM quartic couplings is much too small to be measurable.

[a] The relations are $\mu_W = \frac{e}{2m_W}(2+\Delta\kappa_\gamma+\lambda_\gamma)$ and $Q_W = -\frac{e}{m_W^2}(1+\Delta\kappa_\gamma-\lambda_\gamma)$, respectively.

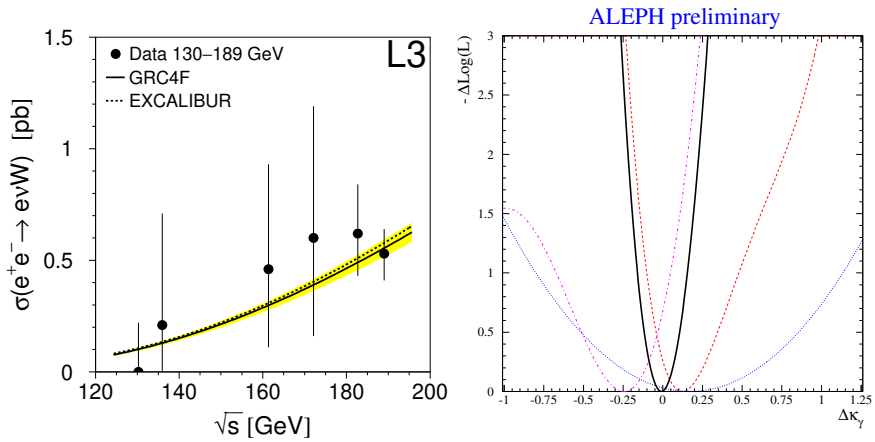

Figure 18. Left: The cross section for single W production as a function of the cms energy as measured by the L3 experiment. Right: Measurement of the triple gauge boson coupling κ_γ by ALEPH. Shown are the likelihood curves obtained from W pairs (dashed line), single W (dashed-dotted) and single photon (dotted) production as well as the sum (solid).

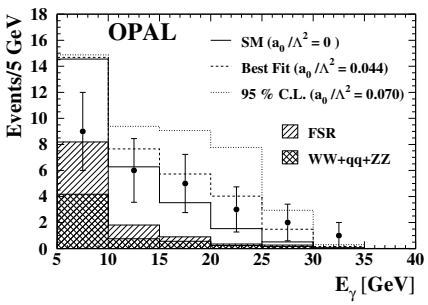

Figure 19. Photon energy spectrum in $e^+e^- \to W^+W^-\gamma$ events as measured by OPAL. The data are compared to the SM and to values of an anomalous quartic coupling parameter a_0/Λ^2 (see Reference [43]) not excluded by the measurement.

Hence only limits on anomalous contributions to the quartic gauge couplings are derived [41,42].

The first analysis of $e^+e^- \to W^+W^-\gamma$ is performed by OPAL and the observed photon spectrum is shown in Figure 19. The photon rate and spectrum is in agreement with the SM calculations and the first direct limits on

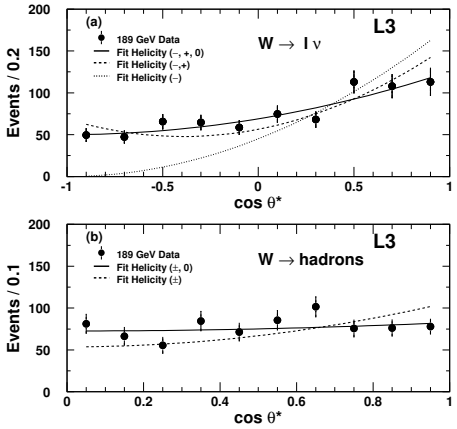

Figure 20. Polar angular distributions in the W boson rest frame as measured by L3. The plot shows the polar angle of the charged lepton in $W \to \ell\nu$ decays (top) and of the jets in hadronic decays (bottom). The lines represent the fit results allowing for transverse polarizations states $(+,-)$ only or including contributions from longitudinal (0) W bosons.

genuine quartic boson couplings [43] are obtained. Also the sensitivity of the reaction $e^+e^- \to \nu\bar{\nu}\gamma\gamma$ to the $WW\gamma\gamma$ vertex is exploited. For some of the coupling parameters more stringent indirect limits exist which are derived from precision measurements at the Z resonance [44].

In addition to the two possible transverse polarization states of massless spin-one particles like the photon, the massive gauge bosons should exist also in the longitudinal helicity state. In the SM this polarization state is related to the mechanism of electroweak symmetry breaking in which three degrees of freedom of the scalar Higgs field generate the longitudinal helicity states of the $W^\pm$ and Z. Remarkably, only transverse W bosons are produced in weak processes involving light fermions. However, in pair production of W bosons at LEP a considerable contribution from longitudinal W bosons is expected [38] making this helicity state experimentally accessible.

The helicity states can be distinguished by the angular distributions of the W decay products. In the rest frame of the W boson the angle between the W and the charged lepton Θ^* follows distributions proportional to $(1 \pm \cos\Theta^*)^2$ for transversely polarized W bosons while longitudinal W bosons produce a $\sin^2\Theta^*$ distribution. Figure 20 shows the measured angular distribution for

leptonic W decays and, symmetrized as no distinction between quarks and anti-quarks is attempted, for hadronic decays. The L3 measurements establish the admixture of longitudinal W bosons. Combining the $\sqrt{s} = 183$ GeV and $\sqrt{s} = 189$ GeV data the fraction of longitudinally polarized W bosons in $e^+e^- \to W^+W^-$ is measured to be [45] $0.261 \pm 0.051 \pm 0.016$ which compares well with the SM expectation of 0.26.

In decays of the heavy top quark 70% of the W bosons are expected to be produced in the longitudinal helicity state. From the observed transverse momentum spectrum in $t \to b\ell\nu$ decays CDF derives this fraction to be [46] $0.91 \pm 0.37 \pm 0.13$ establishing the existence of this helicity state also in top quark decays.

An important measurement performed at LEP II is the precise determination of the mass of the W boson. A first value for m_W was derived from the total cross section measurement at the threshold, $\sqrt{s} = 161$ GeV, which is very sensitive to m_W. The combined LEP result from this measurement is $m_W = 80.40^{+0.22}_{-0.21}$ GeV.

At higher cms energies the W mass is obtained from direct reconstruction of the W decay products. To improve the resolution on the mass, a kinematic fit is performed using the precisely calibrated LEP beam energies. In addition, the masses of the two W bosons in an event are either constrained to be identical or to be the same within the width of the W.

Figure 21 shows examples of the distributions of the reconstructed W mass distributions obtained by the LEP experiments from the 189 GeV data for the four different final states which can be used for this measurement. The data are compared to the result of the fit for m_W, indicating the contributions from the signal and the remaining background, the latter being important only in the four-jet and $q\bar{q}\tau\nu$ channels. Published W mass measurement at LEP can be found in References [47,48,49,50].

A particular problem of the W mass measurement in $e^+e^- \to q\bar{q}\,q\bar{q}$ final states are interactions between the decay products of the two different W bosons: colour reconnection and Bose-Einstein correlations. Because the typical distance between the decay points of the two W bosons (0.1 fm) is much smaller than the hadronisation scale of the quarks (1 fm) gluons are exchanged between quarks from different W bosons implying a momentum transfer and hence a bias in the measurement of the invariant masses. In particular the non-perturbative exchange of soft gluons ($E_g < \Gamma_W$) may have a large impact on the reconstructed W mass.

Mesons consist the main part of hadronisation products of quarks. Obeying Bose-Einstein statistics identical mesons from quark fragmentation tend to occupy the same place in momentum space. Such correlations are experimen-

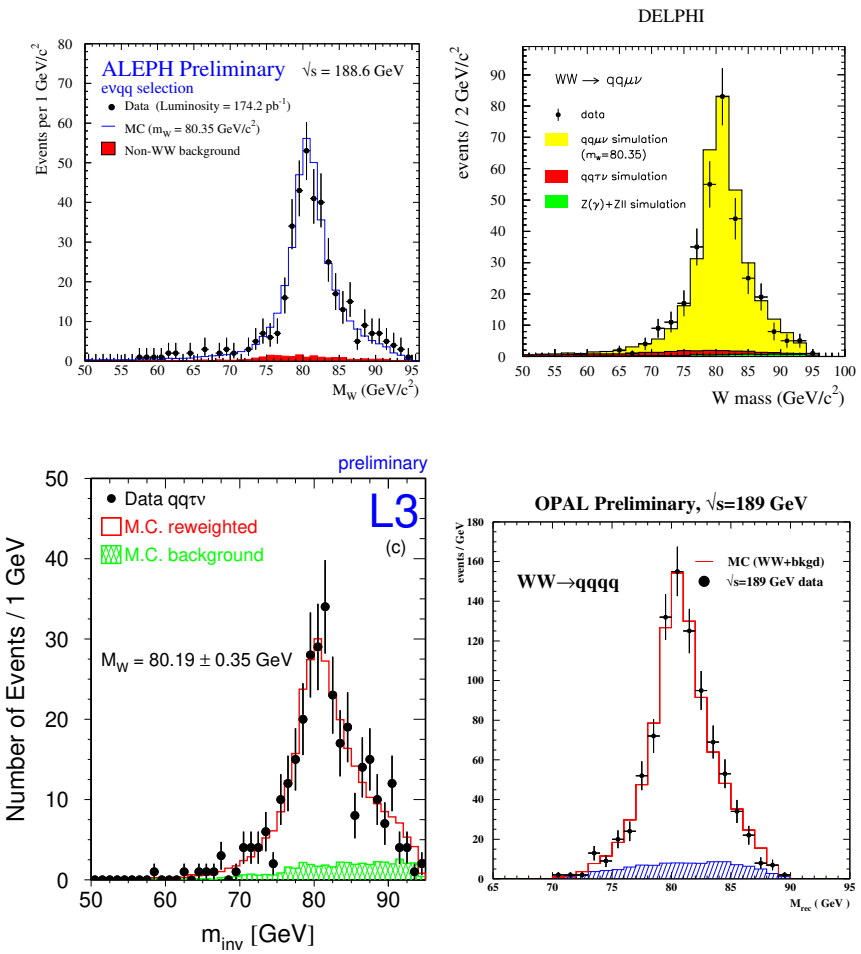

Figure 21. Examples of W mass spectra measured by the LEP experiments in different decay channels.

tally established in hadronic Z and W decays whereas they are not confirmed between mesons stemming from the different W bosons in $e^+e^- \to W^+W^-$. This uncertainty on the existence of possible correlations between mesons from different W bosons, together with the imperfections in their modelling,

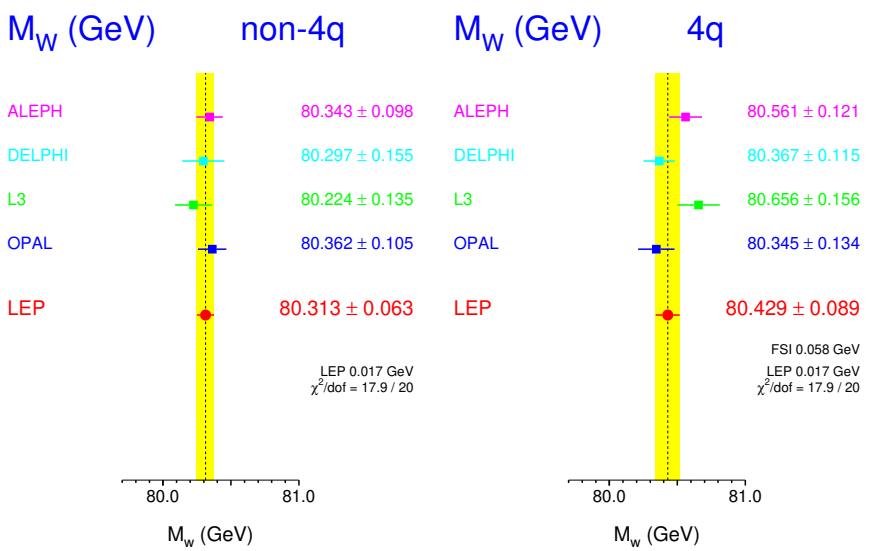

Figure 22. Measurements of the W mass from WW $\to$ $q\bar{q}\,\ell\nu$ (left) and WW $\to$ $q\bar{q}\,q\bar{q}$ (right) at LEP (172 GeV $\leq \sqrt{s} \leq$ 189 GeV). The combined results include correlated errors, in particular from final state interactions and the LEP beam energy calibration.

may lead to a bias in the W mass reconstruction.

Both effects are difficult to model in Monte Carlo simulations. Using the data collected so far, and comparing the fragmentation of W bosons in $q\bar{q}q\bar{q}$ and $q\bar{q}\ell\nu$ events, extreme models can be ruled out. However, the current estimate of the total impact on the W mass measurement in the four-jet channel reaches 58 MeV and consist an important source of the systematic uncertainty.

The results for the W mass obtained at LEP from reconstruction of the decay products are 80.313 ± 0.063 GeV for $q\bar{q}\ell\nu$ and 80.429 ± 0.089 GeV for $q\bar{q}q\bar{q}$ final states, the latter containing a contribution to the error from final state interference effects of 0.058 GeV (Figure 22). Combining all results obtained by the LEP experiments from the data taken from the WW threshold up to $\sqrt{s} = 189$ GeV yields a value for the W mass of

$$m_{\mathrm{W}} = 80.350 \pm 0.056 \text{ GeV}\,. \tag{2}$$

The knowledge of the LEP energy is also important for this mass measurement and its absolute uncertainty contributes by ± 0.017 GeV to the error.

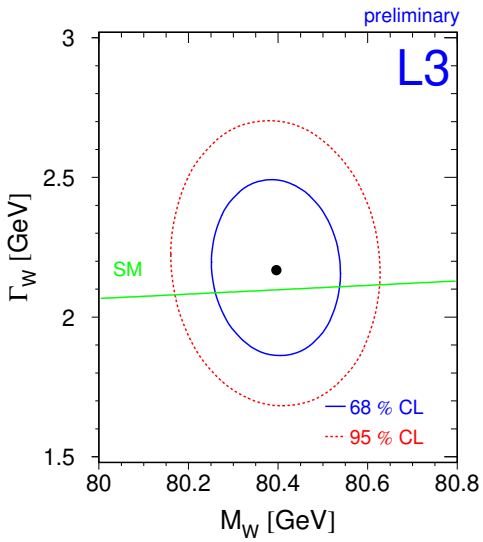

Figure 23. Result of the simultaneous determination of the W mass and width from L3. The central value (dot) and contours obtained from fits to the data are compared to the SM relation (solid line).

When determining the W mass from the measured invariant mass distributions (Figure 21) the total width Γ_W is fixed to the SM prediction. Leaving this parameter free in the fit Γ_W can be determined in a direct way at LEP. As an example Figure 23 shows the result of a simultaneous fit to the W mass and width. The result for the width, $\Gamma_W = 2.12 \pm 0.25$ GeV is found to be in good agreement with the expectation.

5 Tests of the SM of Electroweak Interactions

The measurements of the properties of the heavy gauge bosons, the Z and $W^{\pm}$, discussed above are now used to test the SM of electroweak interactions at the tree level and beyond. Firstly, measurements of the W mass obtained in very different ways are compared. Observables in $e^+e^- \rightarrow f\bar{f}$ at the Z resonance, in particular total cross sections and asymmetries, determine the electroweak couplings. In the SM these couplings are related to the masses of the heavy gauge bosons, immediately evident from the on-shell definition

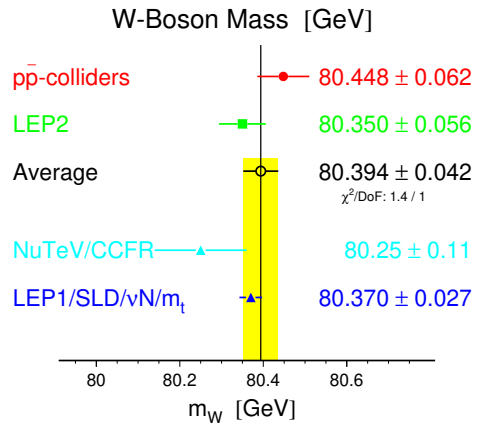

Figure 24. Comparison of W mass measurements. The direct measurements at $p\bar{p}$ colliders and at LEP are averaged and compared to indirect determinations.

of the weak mixing angle $\cos\vartheta_W = m_W/m_Z$. Results of measurements at the Z resonance can thus be converted into a mass of the W boson. It should be noted that m_W enters as parameter in lowest order formulae for observables. To derive the correct value from the measurements inclusion of higher order corrections is however mandatory.

On the other hand at LEP II, as well as at $p\bar{p}$ colliders, the mass of the W boson is directly measured from the invariant mass distribution of its decay products. Mass values from these two approaches are confronted in Figure 24. Their perfect agreement is an experimental confirmation of one of the cornerstones of the SM, namely the double role of the heavy gauge bosons as observable particles with masses determining electroweak couplings. Equivalently, the ratio of the W masses derived from the two approaches consists a measurement of the ρ-parameter which, apart from higher order corrections, is unity in the minimal SM with one Higgs doublet [51].

Furthermore, the experimental data available today allow tests of the SM beyond the tree level investigating higher order corrections. Electroweak radiative corrections Δr arise, among others, from corrections to the gauge boson propagators. They relate the Fermi coupling constant G_F measured at very low momentum transfer from the muon lifetime to the heavy gauge

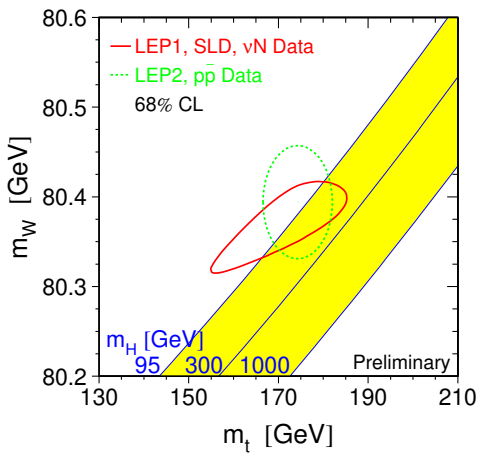

Figure 25. Comparison of direct (dashed contour) and indirect (solid) determinations of the W boson and top quark masses. The solid lines show the SM model relation for three different Higgs boson masses.

boson masses [52]:

$$\frac{G_{\rm F}}{\sqrt{2}} = \frac{\pi\alpha}{2}\,\frac{1}{m_{\rm W}^2 \sin^2\theta_{\rm W}}\,\frac{1}{1-\Delta r}\,. \tag{3}$$

One contribution to the electroweak radiative corrections is the running of the QED coupling constant α which introduces an uncertainty in SM calculations due to the contributions of hadronic loops [53]. Corrections to the $\rm W^{\pm}$ and Z propagators arise from the large mass difference in the third quark doublet which is breaking the isospin symmetry and from Higgs boson loops. As a consequence, observables at the Z resonance depend, in first approximation, quadratically on the top quark mass and on the logarithm of the Higgs mass.

From precise measurements of electroweak observables the mass of the top quark can be inferred to be $m_{\rm t} = 167^{+11}_{-8}$ GeV where the error includes our ignorance of the Higgs mass [33]. This result is in good agreement with the direct measurement [12,54] $m_{\rm t} = 174.3 \pm 5.1$ GeV. Indeed, the mass of the top quark was rather precisely predicted before its discovery in 1994.

A comparison of direct and indirect mass determinations of the W and the top is shown in Figure 25. Very good agreement is observed for both masses

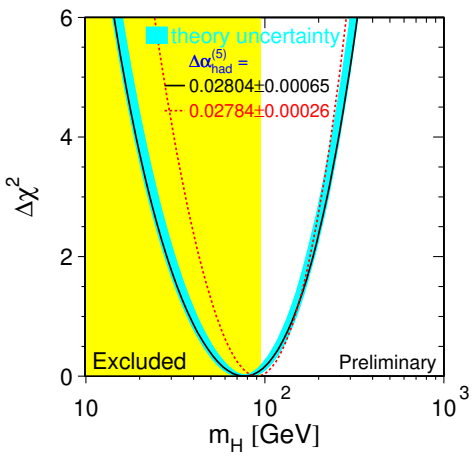

Figure 26. Result of the SM fit to all electroweak precision data. The solid line shows the dependence of the χ^2 on the Higgs boson mass with the estimated theoretical error on the calculation indicated by the band. The dashed line represents the result of the fit using the determination of $\Delta\alpha^{(5)}_{\rm had}$ of reference [55]. The shaded region at the left is excluded by the search for Higgs boson production at LEP.

and the conclusion is that the SM is correct at the 1-loop level. Also shown in Figure 25 is the SM prediction using the relation between $G_{\rm F}$ and $m_{\rm W}$ (Equation 3) for different Higgs masses ranging from the lower experimental bound (see Section 6) to the upper theoretical limit[b]. Note that the precise measurements of electroweak observables indicate a low mass for the SM Higgs boson.

This mass is determined in a fit to all available electroweak measurements. As the weak radiative corrections depend quadratically on the mass of the top quark its direct determination at the Tevatron is important for the determination of $m_{\rm H}$. This fit yields an estimate for the Higgs mass in the SM and an upper limit of [33]:

$$m_{\rm H} = 77^{+69}_{-39}\ {\rm GeV} \qquad m_{\rm H} < 215\ {\rm GeV}\,. \tag{4}$$

The asymmetric errors reflect the logarithmic dependence of electroweak

[b]The lower limit on the Higgs mass used here, $m_{\rm H} > 95$ GeV, is obtained at LEP from data up to $\sqrt{s} = 189$ GeV.

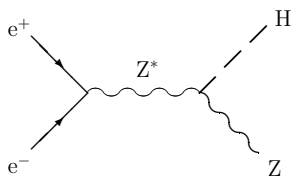

Figure 27. Feynman diagram of the Higgs-strahlung process which would be the main production mechanism for the SM Higgs at LEP II.

observables on the Higgs mass. The χ^2 of this fit as function of m_{H} is shown in Figure 26. The band indicates the estimated theoretical uncertainty which contributes to about ± 5 GeV to the errors of Equation 4. Also shown in Figure 26 is the χ^2 curve when a more theory dependent calculation of the hadronic contribution to the running of the QED coupling constant α is used [55]. The lower limit on m_{H} obtained from the direct search for the Higgs boson at LEP is shown as well.

6 Search for Higgs Bosons at LEP

Before the startup of the LEP collider in 1989 experiments were only sensitive to very small Higgs boson masses and the limits derived were subject to large uncertainties [56]. The experiments performed at LEP search for the production of the Higgs boson in electroweak processes which are readily calculable and do not suffer from large theoretical uncertainties. In addition, the LEP collider is a copious source of a heavy particle, the Z boson, which ensures sizeable Higgs production cross sections. For these reasons the LEP experiments have eclipsed previous experimental limits such that at the end of the running at the Z resonance in 1995 the entire mass range for the SM Higgs boson $0 \leq m_{\mathrm{H}} \leq 63.9$ GeV [57] could be excluded.

With the increase of the cms energy the search for the SM Higgs boson continues now for larger mass values. The production of SM Higgs bosons at LEP II would proceed mainly through the Higgs-strahlung diagram shown in Figure 27 with small contributions from WW and ZZ fusion. The range of masses which can be explored at a given cms energy is then limited by the fact that the Higgs boson is produced in conjunction with a real Z boson. Below this kinematic threshold the cross section $\mathrm{e^+e^-} \rightarrow \mathrm{ZH}$ rises quickly to a sizeable level as compared to other SM processes. This results in a much better signal to background ratio as compared to the searches performed at

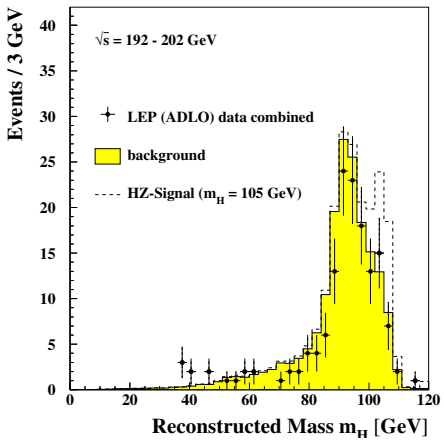

Figure 28. Combined mass distribution of candidate events obtained by the four LEP experiments in the search for the SM Higgs boson in 1999 [62]. The data are compared to the background from other SM processes and the hypothetical production of Higgs bosons with $m_{\mathrm{H}} = 105$ GeV.

the Z resonance.

Following the decay modes of the Z and Higgs bosons four final states are distinguished. In the mass range investigated the Higgs boson decays predominantly into b quarks ($\approx 85\%$), but also its decays into tau leptons and other quarks are considered: (i) $\mathrm{HZ} \to \mathrm{b\bar{b}\,q\bar{q}}$ (four jets); (ii) $\to \mathrm{b\bar{b}}\,\nu\bar{\nu}$ (two acoplanar jets); (iii) $\to \mathrm{b\bar{b}\,e^+e^-}$, $\mathrm{b\bar{b}}\,\mu^+\mu^-$ (two jets and two leptons) and (iv) $\to \tau^+\tau^-\,\mathrm{q\bar{q}}$. The main backgrounds are fermion-pair production, in particular $\mathrm{e^+e^-} \to \mathrm{q\bar{q}}$, four fermion final states from $\mathrm{e^+e^-} \to \mathrm{W^+W^-}$ and $\mathrm{e^+e^-} \to \mathrm{ZZ}$ and for $\mathrm{H}\,\nu\bar{\nu}$ the production of single W bosons $\mathrm{e^+e^-} \to \mathrm{We}\nu$.

The most sensitive channel in the Higgs search is the four-jet topology due to the high hadronic branching ratio of the Z. The tagging of b quarks is essential in all decay channels to suppress background. Kinematic fits are employed to improve the mass resolution on the hypothetical Higgs boson in candidate events. The fits exploit the fact that the two objects, jets or leptons, not associated to the Higgs boson should stem from a real Z boson. The analyses employed in the search for the SM Higgs boson are described in References [58,59,60,61].

No indication for Higgs boson production is observed at LEP so far up

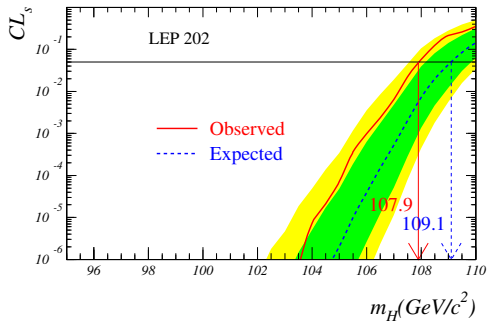

Figure 29. The confidence level for the hypothesis of Higgs boson production as a function of m_{H} obtained from the combination of the LEP experiments. The expected curve is shown as the median of Monte Carlo trials together with bands indicating the ranges which contain 68% and 95% of these trials.

to a cms energy of 202 GeV [62]. An illustration of the negative search result is given in Figure 28 which shows the reconstructed mass distribution of the best candidate events of the four experiments compared to the background expectation and the hypothetical production of Higgs bosons with a mass of 105 GeV.

Therefore, only a lower mass limit can be derived from the data. The hypothesis of Higgs boson production, with respect to the presence of background only, is tested as a function of m_{H} taking into account candidate events and their significance for a given mass value. Figure 29 shows the confidence level CL_S for the presence of the signal as a function of m_{H} as obtained from the combination of the four experiments. In addition to the measured CL_S the expected confidence level is also shown. It is derived from a large number of Monte Carlo experiments simulating the data samples and detector performances in the background-only hypothesis. From the intersection of the observed CL_S with the 5% line the lower limit for the mass of the SM Higgs boson is derived to be [62]:

$$m_{\mathrm{H}} > 107.9 \text{ GeV} \qquad 95\%\text{CL} \tag{5}$$

In SUSY models the Higgs sector consists of more than one fundamental scalar particle. At least two Higgs doublets are necessary to create masses for all fermions and their scalar partners. Therefore, in the Minimal Supersymmetric (MSSM) extension of the SM (see also Section 7) five Higgs bosons are predicted: H^+, H^-, H, h and A, where h is believed to be the lightest one. In this model the charged Higgs bosons are heavier than the W and beyond the

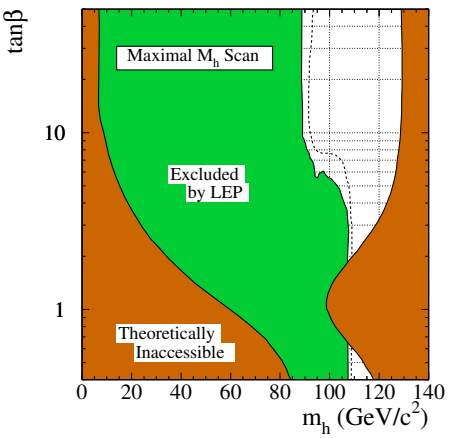

Figure 30. Excluded region in the $m_{\mathrm{h}} - \tan\beta$ plane from the combination of the LEP experiments. The shaded regions on the right and left side of the plot are theoretically inaccessible.

reach of the LEP experiments.

The experiments search for the production of the two additional neutral bosons in the reactions $\mathrm{e^+e^-} \to \mathrm{hA}$ and $\mathrm{e^+e^-} \to \mathrm{hZ}$. The cross sections of these processes depend on the parameter $\tan\beta$, the ratio of the vacuum expectation values associated to the two Higgs doublets. The production of hA is dominant for large $\tan\beta$ values whereas the reaction $\mathrm{e^+e^-} \to \mathrm{hZ}$, with an experimental signature very similar to the SM Higgs boson production discussed above, governs at low $\tan\beta$.

No evidence for the production of h or A bosons is observed so far at LEP. Lower mass limits are derived for the neutral MSSM Higgs bosons as function of $\tan\beta$. The combined LEP result for the h boson is shown in Figure 30. The limit obtained for small $\tan\beta$ is the same as for the SM Higgs boson and it decreases for larger values of $\tan\beta$. The lower experimental mass limits for the neutral MSSM Higgs bosons h and A for any $\tan\beta$ are:

$$m_{\mathrm{h}} > 88.3 \text{ GeV} \qquad m_{\mathrm{A}} > 88.4 \text{ GeV}\,. \tag{6}$$

Also shown in Figure 30 are regions in the plane of $\tan\beta$ and m_{h} which

are not allowed by the theory.[c] Comparing this to the experimental limit on m_{h} the region $0.7 < \tan\beta < 1.8$ is excluded. However, the searches for the neutral MSSM Higgs bosons assume that they predominantly decay into b-quarks which is not necessarily the case for all choices of the model parameters. Studies are under way to include other experimental results in order to possibly generalize the $\tan\beta$ exclusion.

Searches for charged Higgs bosons as well as Higgs bosons not decaying in a standard manner are performed by the LEP collaborations without finding any evidence for their existence. Examples of these analyses and results can be found in References [63,64,65,66].

7 Search for Supersymmetric Particles at LEP

In addition to the search for the production of SUSY Higgs bosons searches for new particles predicted by SUSY theories [3] are carried out by the LEP experiments. These theories predict the existence of scalar partners of the known quarks, $\tilde{\mathrm{q}}$, and leptons, $\tilde{\ell}^{\pm}$, $\tilde{\nu}$, as well as fermionic partners of the gauge and Higgs bosons. The neutral partners of the bosons mix into four mass eigenstates, called neutralinos, $\tilde{\chi}_i^0$, with the index ordering them by mass. The partners of the charged bosons form two chargino mass eigenstates, the lighter one denoted as $\tilde{\chi}_1^{\pm}$.

Three different type of models are investigated which can be distinguished by the type and nature of the lightest SUSY particle (LSP): (i) gravity mediated SUSY breaking with a heavy gravitino $\tilde{\mathrm{G}}$ and the LSP being the lightest neutralino $\tilde{\chi}_1^0$; (ii) gauge mediated SUSY breaking with the $\tilde{\mathrm{G}}$ as LSP; (iii) R-parity violating SUSY in which the LSP is unstable.

Up to the highest cms energy no sign for SUSY is observed at LEP. A few examples of search results on the first two scenarios are discussed here. Recently published results on searches for SUSY particles can be found in References [67,68,69,70].

At LEP the production and decay of charginos, neutralinos and scalar leptons and quarks would take place by the reactions listed in Table 3. With only these assumptions on the production and decay of SUSY particles upper limits on production cross sections are derived from the data.

As an example Figure 31 shows the experimental upper limit on the cross section $\mathrm{e^+e^-} \to \tilde{\chi}_1^+\tilde{\chi}_1^-$ at 189 GeV obtained by L3. The most constraining

[c] The calculations are done for $m_{\mathrm{t}} = 174.3$ GeV, the MSSM parameters $M_{\mathrm{SUSY}} = 1$ TeV, $M_2 = 200$ GeV and the scalar top mixing is chosen such that the theoretically allowed value for m_{h} is maximal.

Table 3. Production and decay of SUSY particles as studied by the LEP experiments assuming R-parity conservation.

Production	Decay
$e^+e^- \to \tilde{\chi}_i^0\tilde{\chi}_j^0$	$\tilde{\chi}_i^0 \to \tilde{\chi}_1^0 ff,\ \tilde{\chi}_1^0\gamma \quad (i>1)$
$e^+e^- \to \tilde{\chi}_1^+\tilde{\chi}_1^-$	$\tilde{\chi}_1^\pm \to \tilde{\chi}_1^0 q\bar{q},\ \tilde{\chi}_1^0\ell^\pm\nu,\ \tilde{\nu}\ell^\pm$
$e^+e^- \to \tilde{\ell}^+\tilde{\ell}^-$	$\tilde{\ell}^\pm \to \tilde{\chi}_1^0\ell^\pm$
$e^+e^- \to \tilde{q}\,\tilde{q}$	$\tilde{t}_1 \to \tilde{\chi}_1^0 c,\quad \tilde{b}_1 \to \tilde{\chi}_1^0 b$

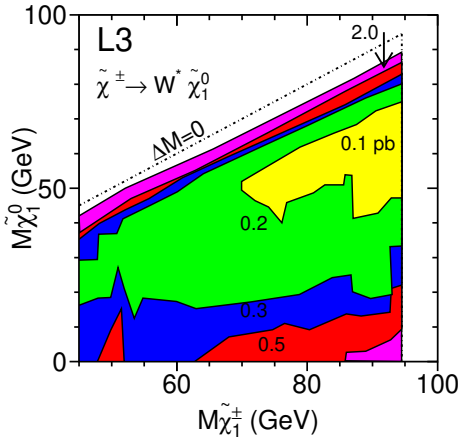

Figure 31. Upper experimental bounds on the cross section $e^+e^- \to \tilde{\chi}_1^+\tilde{\chi}_1^-$ at $\sqrt{s} = 189$ GeV obtained by the L3 experiment as function of the chargino and neutralino masses.

upper limit, $\sigma_{\tilde{\chi}_1^+\tilde{\chi}_1^-} < 0.1$ pb, is obtained in the region $m_{\tilde{\chi}_1^\pm} \approx 90$ GeV and $m_{\tilde{\chi}_1^0} \approx 60$ GeV where the kinematic conditions are favourable providing high detection efficiency and good background suppression for the signatures given in Table 3. Limits on the cross section become worse as the neutralino mass approaches the mass of the chargino because the visible energy in the detector decreases which reduces the detection efficiency. Also background from two-photon processes is important here. Similarly, if the mass difference between chargino and neutralino is large the missing energy is reduced and chargino events resemble more and more SM background like W-pair production. This makes background suppression difficult and consequently only higher cross sections can be excluded. Chargino masses below 45 GeV are ruled out by

measurements at the Z resonance. The region above the dashed line is kinematically not allowed by requiring that the neutralino is lighter than the chargino. Similar results are obtained for the production cross sections of scalar leptons.

Recently the LEP experiments have developed analyses to explore the region where the mass difference between the chargino and the neutralino is small. Signatures with accompanying initial state bremsstrahlung are investigated to suppress the background from two-photon interactions [71,72]. If the chargino and neutralino are nearly mass degenerated the chargino has a very long lifetime and could be recognized in the detectors as a stable, heavy charged particle. No signal has been observed in these two types of searches. As a result chargino production at LEP is ruled out independently of the mass difference to the neutralino.

The upper limit on production cross sections on SUSY particles are now interpreted in the framework of the MSSM. The free parameters are the gaugino mass at the weak scale M_2, the mass scale of the scalar partners of the fermions m_0, the mixing parameter of the two Higgs field doublets μ, the tri-linear coupling parameter A and $\tan\beta$. Values around $\tan\beta = 1.5$ and 35 are favoured by cosmological arguments.

In the MSSM high cross sections of the order of several picobarn are expected for a wide range of parameter space in the kinematically accessible region at LEP II, in particular for chargino pair production. Expected cross sections at $\sqrt{s} = 189$ GeV as a function of the chargino mass are shown in Figure 32. The two bands shown, obtained from MSSM parameter variations, correspond to a high scalar neutrino mass $m_{\tilde{\nu}}$ and to the lowest mass compatible with the limit obtained at LEP I. The chargino is assumed to be 10 GeV or 5 GeV heavier than the invisible LSP. The expected cross section depends on $m_{\tilde{\nu}}$ because the t-channel exchange of scalar neutrinos interferes destructively with the s-channel boson exchange and it reaches a minimum for $m_{\tilde{\nu}} \approx 100$ GeV. From the non-observation of a signal upper limits on the chargino production cross section are set and converted into lower mass limits which are in some cases close to the kinematic limit.

Mass limits on scalar top and bottom quarks are presented in Figure 33 as obtained by the DELPHI experiment. Mass eigenstates of scalar top and bottom quarks are superpositions of the scalar partners of the left- and right-handed quarks, e.g. $\tilde{t}_1 = \tilde{t}_L \cos\Theta_{\mathrm{LR}} + \tilde{t}_R \sin\Theta_{\mathrm{LR}}$. The coupling of the $\tilde{t}_1$ to the Z depends on the mixing angle Θ_{LR} and for a value of $\cos\Theta_{\mathrm{LR}} = 0.57$ the scalar top decouples from the Z leading to a minimal production cross section. In this case the derived mass limit on the scalar top is lower as compared to the case of no mixing, i.e. assuming that the mass eigenstate corresponds to

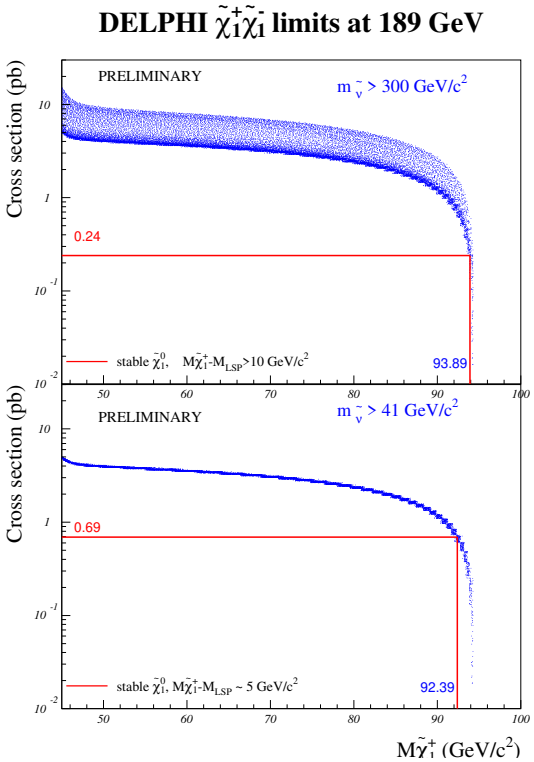

Figure 32. Expected MSSM cross section for chargino pair production at 189 GeV for large and small chargino-neutralino mass differences. The experimental upper limits on the cross sections are indicated from which chargino mass limits are derived.

the scalar partner of the left-handed top quark. Similarly, mass limits for a scalar bottom quark are shown for these two scenarios in Figure 33. To obtain these limits 100% branching ratios into $\tilde{t}_1 \to c\tilde{\chi}_1^0$ and $\tilde{b}_1 \to b\tilde{\chi}_1^0$ are assumed.

The lightest neutralino is a candidate for the dark matter in the universe. Therefore, a lower limit on $m_{\tilde{\chi}_1^0}$ valid for all choices of MSSM parameter is particularly interesting. From scanning the MSSM parameter space the LEP experiments obtain values for this absolute limit in the vicinity of 30 GeV, for instance $m_{\tilde{\chi}_1^0} > 32.5$ GeV is obtained by L3. This result is illustrated in Figure 34 where the lower mass limit is shown as a function of $\tan\beta$ for all choices of m_0. The same analysis yields also an absolute lower limit on the

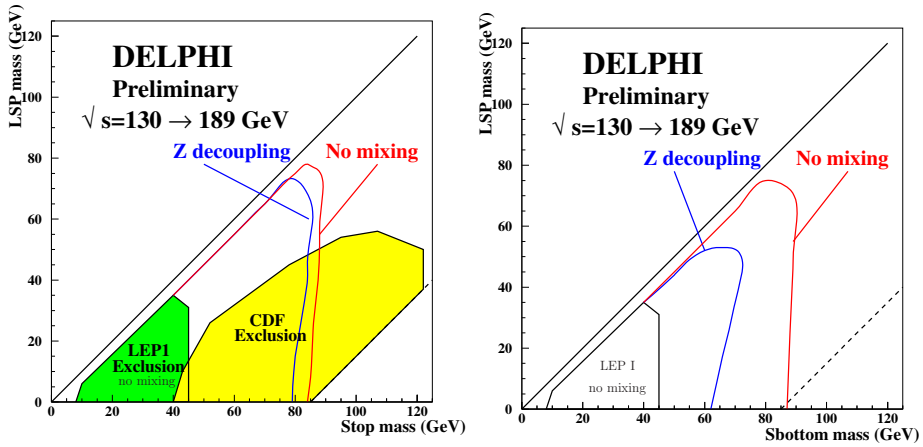

Figure 33. Exclusion region in the $\tilde{\chi}_1^0 - \tilde{t}_1$ and $\tilde{\chi}_1^0 - \tilde{b}_1$ planes. The results obtained by DELPHI at high cms energies are compared to the result derived from data at the Z resonance and, for the scalar top, to a search performed in $p\bar{p}$ collisions.

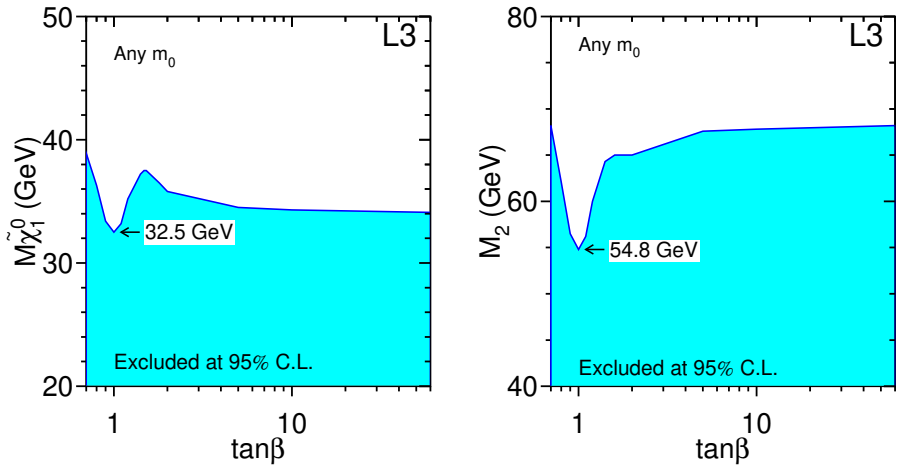

Figure 34. Lower mass limits for the neutralino and the chargino obtained by L3 as a function of $\tan\beta$ from a scan in the MSSM parameter space.

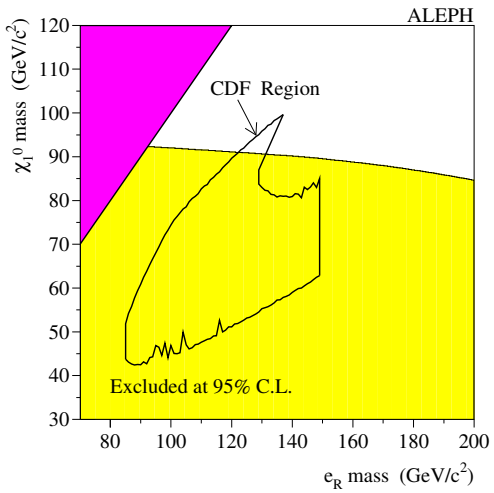

Figure 35. Excluded region in the $m_{\tilde{\chi}_1^0} - m_{\tilde{e}}$ plane from the study of di-photon events with missing energy obtained by ALEPH. The kinematically allowed region of a CDF event which can be interpreted by the production of scalar electrons is shown for comparison [73].

chargino mass in the MSSM of $m_{\tilde{\chi}_1^\pm} > 54.8$ GeV.

Gauge mediated SUSY breaking models in which the gravitino is light can be investigated at LEP in studies of photonic final states. Processes like $e^+e^- \to \tilde{G}\tilde{G}\gamma$ or $e^+e^- \to \tilde{G}\tilde{G} \to \tilde{\chi}_1^0\tilde{\chi}_1^0\gamma\gamma$ lead to one or more photons visible in the detector and nothing else. Also in the MSSM production of heavier neutralinos and their subsequent radiative decay would produce this experimental signature. In the SM the reaction $e^+e^- \to \nu\bar{\nu}\gamma(\gamma)$ gives rise to final states with photons and missing energy. The observed photon spectra agree in total rate as well as in shape with the SM expectation, e.g. Figure 5, and do not necessitate contributions from SUSY processes.

The study of di-photon events can be used to set upper limits on the cross section for the process $e^+e^- \to \tilde{\chi}_1^0\tilde{\chi}_1^0 \to \tilde{G}\tilde{G}\gamma\gamma$ and to interpret them in terms of mass limits for SUSY particles. The excluded mass of the lightest neutralino as a function of the scalar electron mass is shown in Figure 35. It is compared to the kinematic region of an event observed by CDF [73] which could be explained by the production of scalar electrons [74]. Almost the entire region is excluded now by the LEP experiments proving unlikely this interpretation.

8 Conclusions and Outlook

The LEP collider and the four experiments have been operated successfully at cms energies from the Z resonance up to 202 GeV. Many precise measurements are performed with the large amount of data collected, for example the determination of the properties of the Z and W bosons. The SM of electroweak and strong interactions is confirmed up to the highest energy reached in e^+e^--collisions so far.

The increase in energy opens new kinematic regions in the search for new particles. No sign of Higgs boson production or of SUSY particles is observed by the experiments. The negative search results yield many improved lower mass limits. For instance, the SM Higgs boson must be heavier than 107.9 GeV if it exists.

In the year 2000, the last year of LEP operation, the energy of the collider will be further increased. The main emphasis will be the search for new particles in the extended kinematic range. For example the SM Higgs boson could be discovered up to masses exceeding 110 GeV.

Acknowledgements

I would like to thank the organisers of the XXVIII International Meeting on Fundamental Physics for their invitation and their hospitality. Many colleagues from the LEP experiments helped me to compile the results from the recent run. Also, I am grateful to S. Roth for the careful reading of the manuscript.

References

1. S.L. Glashow, Nucl. Phys. **22** (1961) 579; S. Weinberg, Phys. Rev. Lett. **19** (1967) 1264; A. Salam, "Elementary Particle Theory", Ed. N. Svartholm, Stockholm, "Almquist and Wiksell" (1968), 367.
2. P.W. Higgs, Phys. Lett. **B 12** (1964)132; F. Englert and R. Brout, Phys. Rev. Lett. **13** (1964) 321; G.S. Guralnik *et al*, Phys. Rev. Lett. **13** (1964) 585.
3. P. Fayet, Phys. Lett. **B 64** (1976) 156, Phys. Lett. **B 69** (1977) 489; P. Fayet and S. Ferrara, Phys. Rep. **32** (1977) 249; H.P. Nilles, Phys. Rep. **110** (1984) 1; H. Haber and G. Kane, Phys. Rep. **117** (1985) 75.
4. D. Bardin *et al*, "ZFITTER v.6.21, A Semi-Analytical Program for Fermion-Pair Production in e^+e^- Annihilation", Preprint DESY 99-070, hep-ph/9908433; P. Christova, M. Jack and T. Riemann, Phys. Lett. **B**

456 (1999) 264; D. Bardin *et al*, Phys. Lett. **B 255** (1991) 290 and CERN-TH 6443/92 (May 1992); Nucl. Phys. **B 351**(1991) 1; Comp. Phys. Comm. **59** (1990) 303; Z. Phys. **C 44** (1989) 493.
5. G. Montagna *et al*, Nucl. Phys. **B 401** (1993) 3; Comp. Phys. Comm. **76** (1993) 328.
6. ALEPH Collab., R. Barate *et al*, E. Phys. J. **C 12** (1999) 183.
7. DELPHI Collab., P. Abreu *et al*, "Measurement and Interpretation of Fermion-Pair Production at LEP2 Energies of 183 and 189 GeV", Preprint CERN-EP-2000-068, CERN, 2000, submitted to Phys. Lett. B.
8. L3 Collab., M. Acciarri *et al*, Phys. Lett. **B 479** (2000) 101.
9. OPAL Collab., G. Abbiendi *et al*, E. Phys. J. **C 13** (2000) 553.
10. L3 Collab., M. Acciarri *et al*, Phys. Lett. **B 470** (1999) 268.
11. J. Mnich, "Tests of the Standard Model", Proceedings of the International Europhysics Conference on High Energy Physics 99, Tampere, Finland, eds. K. Huitu, H Kurki-Suonio and J. Maalampi.
12. Particle Data Group, D.E. Groom *et al*, "Review of Particle Physics", E. Phys. J. **C 15** (2000) 1.
13. DELPHI Collab., P. Abreu *et al*, E. Phys. J. **C 11** (1999) 383.
14. L3 Collab., M. Acciarri *et al*, Phys. Lett. **B 485** (2000) 71.
15. OPAL Collab., G. Abbiendi *et al*, E. Phys. J. **C 16** (2000) 41.
16. E. Eichten, K. Lane and M. Peskin, Phys. Rev. Lett. **50** (1983) 81.
17. For reviews see for instance:
    J.L. Hewett and T.G. Rizzo, Phys. Rev. **183** (1989) 193; L.S. Durkin and P. Langacker, Phys. Lett. **B 166** (1986) 436; R.N. Mohapatra, "Unificaion and Supersymmetries", Springer, New York 1989.
18. L3 Collab., M. Acciarri *et al*, "QCD Studies in e^+e^- Annihilation from 30 GeV to 189 GeV", Preprint CERN-EP-2000-064, CERN, 2000, submitted to Phys. Lett. B.
19. ALEPH Collab., R. Barate *et al*, Phys. Lett. **B 429** (1998) 201.
20. DELPHI Collab., P. Abreu *et al*, Phys. Lett. **B 433** (1998) 429.
21. L3 Collab., M. Acciarri *et al*, Phys. Lett. **B 475** (2000) 198.
22. OPAL Collab., G. Abbiendi *et al*, Phys. Lett. **B 465** (1999) 303.
23. L3 Collab., M. Acciarri *et al*, Phys. Lett. **B 439** (1998) 183.
24. OPAL Collab., G. Abbiendi *et al*, Phys. Lett. **B 438** (1998) 391.
25. ALEPH Collab., R. Barate *et al*, Phys. Lett. **B 469** (1999) 287.
26. DELPHI Collab., P. Abreu *et al*, "Measurement of the ZZ cross-section in e^+e^- interactions at 183-189 GeV", Preprint CERN-EP-2000-089, CERN, 2000, submitted to Phys. Lett. B.
27. L3 Collab., M. Acciarri *et al*, Phys. Lett. **B 465/1-4** (1999) 363.
28. OPAL Collab., G. Abbiendi *et al*, Phys. Lett. **B 476** (2000) 256.

29. ALEPH Collab., R. Barate *et al*, "Measurement of W-pair production in e^+e^- Collisions at 189 GeV", Preprint CERN-EP-2000-052, CERN, 2000, submitted to Phys. Lett. B.
30. DELPHI Collab., P. Abreu *et al*, "W pair production cross-section and W branching fractions in e^+e^- interactions at 189 GeV", Preprint CERN-EP-2000-035, CERN, 2000, submitted to Phys. Lett. B.
31. L3 Collab., M.Acciarri *et al.*, "Measurement of the W-pair Production Cross Section and W-Decay Branching Fractions in e^+e^- Interactions at $\sqrt{s} = 189$ GeV", Preprint CERN-EP/2000-104, CERN, 2000, submitted to Phys. Lett. B.
32. OPAL Collab., G. Abbiendi *et al*, E. Phys. J. **C 8** (1999) 191.
33. The LEP Collaborations, ALEPH, DELPHI, L3, OPAL, the LEP Electroweak Working Group and the SLD Heavy Flavour Group and Electroweak Groups, "A Combination of Preliminary Electroweak Measurements and Constraints on the Standard Model", Preprint CERN-EP/2000-016, CERN, 2000.
34. N. Cabbibo, Phys. Rev. Lett. **10** (1963) 531.
35. M. Kobayashi and M. Maskawa, Prog. Theor. Phys. **49** (1963) 652.
36. W. Beenakker *et al*, in "Physics at LEP 2", Report CERN 96-01 (1996), eds. G. Altarelli, T. Sjöstrand, F. Zwirner, Vol. 1, p. 79
37. K. Hagiwara *et al*, Nucl. Phys. **B 282** (1987) 253.
38. G. Gounaris *et al*, in "Physics at LEP 2", Report CERN 96-01 (1996), eds. G. Altarelli, T. Sjöstrand, F. Zwirner, Vol. 1, p. 525
39. ALEPH Collab., R. Barate *et al*, Phys. Lett. **B 462** (1999) 389.
40. L3 Collab., M. Acciarri *et al*, "Production of Single W Bosons at $\sqrt{s}$ = 189 GeV and Measurements of WWγ Gauge Couplings", Preprint CERN-EP/2000-066, CERN, 2000, submitted to Phys. Lett. B.
41. L3 Collab., M. Acciarri *et al*, "Measurement of the $W^+W^-\gamma$ Cross Section and Direct Limits on Anomalous Quartic Gauge Boson Couplings at LEP", Preprint CERN-EP/2000-097, CERN, 2000, submitted to Phys. Lett. B.
42. OPAL Collab., G. Abbiendi *et al*, Phys. Lett. **B 471** (1999) 293.
43. G. Bélanger and F. Boudjema, Phys. Lett. **B 288** (1992) 201.
44. O. Eboli, M. Gonzaléz and S. Novaes, Nucl. Phys. **B 411** (1994) 381.
45. L3 Collab., M. Acciarri *et al*, Phys. Lett. **B 474** (1999) 194.
46. CDF Collab., T. Affolder *et al*, "Measurement of the Helicity of W Bosons in Top Quark Decays ", Preprint FERMILAB-PUB-99/257-E, FERMILAB, 1999, submitted to Phys. Rev. Lett.
47. ALEPH Collab., R. Barate *et al*, "Measurement of the W Mass and Width in e^+e^- Collisions at 189 GeV", Preprint CERN-EP-2000-045,

CERN, 2000, submitted to E. Phys. J. C.
48. DELPHI Collab., P. Abreu *et al*, Phys. Lett. **B 462** (1999) 410.
49. L3 Collab., M. Acciarri *et al*, Phys. Lett. **B 454** (1999) 386.
50. OPAL Collab., G. Abbiendi *et al*, Phys. Lett. **B 453** (1999) 138.
51. M. Veltman, Nucl. Phys. **B 123** (1977) 89; M.S. Chanowitz *et al*, Phys. Lett. **B 78** (1978) 1; M. Consoli, S. Lo Presti, L. Maiani, Nucl. Phys. **B 223** (1983) 474; J. Fleischer, F. Jegerlehner, Nucl. Phys. **B 228** (1983) 1.
52. A. Sirlin, Phys. Rev. **D 22** (1980) 971, Phys. Rev. **D 29** (1984) 89; W.J. Marciano and A. Sirlin, Phys. Rev. **D 29** (1984) 945.
53. S. Eidelman and F. Jegerlehner, Z. Phys. **C 67** (1995) 585.
54. CDF Collab., F. Abe *et al*, Phys. Rev. Lett. **82** (1998) 271; Phys. Rev. Lett. **82** (1998) 2808; Phys. Rev. Lett. **80** (1998) 2767; DØCollab., B. Abbott *et al.*, Phys. Rev. Lett. **80** (1998) 2063; Phys. Rev. **D 58** (1998) 052001; Phys. Rev. **D 60** (1999) 052001.
55. M. Davier and A. Höcker, Phys. Lett. **B 419** (1998) 419.
56. M. Aiguilar-Benitez *et al*, "The 1988 Review of Particle Physics", Phys. Lett. **B 204** (1988) 1.
57. S. Park, in 10th Topical Workshop of Proton-Antiproton Collider Physics, eds. R. Raja and G. Yoh, AIP Press, New York 1995.
58. ALEPH Collab., R. Barate *et al*, "Search for neutral Higgs bosons of the Standard Model and the MSSM in e^+e^- collisions at $\sqrt{s} = 189$ GeV", Preprint CERN-EP-2000-019, CERN, 2000, submitted to E. Phys. J. C.
59. DELPHI Collab., P. Abreu *et al*, "Searches for Neutral Higgs Bosons in e^+e^- Collisions around $\sqrt{s} = 189$ GeV", Preprint CERN-EP-2000-038, CERN, 2000, submitted to E. Phys. J. C.
60. L3 Collab., M. Acciarri *et al*, Phys. Lett. **B 461** (1999) 376.
61. OPAL Collab., G. Abbiendi *et al*, E. Phys. J. **C 12** (2000) 567.
62. The LEP Collaborations, ALEPH, DELPHI, L3, OPAL, the LEP Electroweak Working Group for Higgs boson searches, "Searches for Higgs bosons: Preliminary combined results using LEP data collected at energies up to 202 GeV", Preprint CERN-EP/2000-055, CERN, 2000.
63. ALEPH Collab., R. Barate *et al*, "Search for charged Higgs bosons in e^+e^- Collisions at energies up to $\sqrt{s} = 189$ GeV", Preprint CERN-EP-2000-086, CERN, 2000, submitted to Phys. Lett. B; Phys. Lett. **B 466** (1999) 50; "Search for $\gamma\gamma$ decays of a Higgs boson produced in association with a fermion pair e^+e^- collisions at LEP", Preprint CERN-EP-2000-083, CERN, 2000, submitted to Phys. Lett. B.
64. DELPHI Collab., P. Abreu *et al*, Phys. Lett. **B 460** (1999) 484; "A search for invisible Higgs bosons produced in e^+e^- interactions up to $\sqrt{s}$

= 189 GeV", Preprint CERN-EP-2000-051, CERN, 2000, submitted to Phys. Lett. B.
65. L3 Collab., M. Acciarri *et al*, "Search for Charged Higgs Bosons in e^+e^- Collisions at Centre-of-Mass Energies up to 202 GeV", Preprint CERN-EP/2000-118, CERN, submitted to Phys. Lett. B; Phys. Lett. **B 485** (2000) 85.
66. OPAL Collab., G. Abbiendi *et al*, "Two Higgs Doublet Model and Model Independent Interpretation of Neutral Higgs Boson Searches", Preprint CERN-EP-2000-092, CERN, 2000, submitted to Eur. Phys. J; Phys. Lett. **B 464** (1999) 311.
67. ALEPH Collab., R. Barate *et al*, Phys. Lett. **B 469** (1999) 303; "Search for Gauge Mediated SUSY Breaking Topologies collisions at $\sqrt{s}$ = 189 GeV, Preprint CERN-EP/99-171, CERN, 1999, submitted to E. Phys. J. C; Phys. Lett. **B 488** (2000) 234.
68. DELPHI Collab., P. Abreu *et al*, Phys. Lett. **B 466** (1999) 61; "Search for charginos in e^+e^- interactions at $\sqrt{s}$ = 189 GeV", Preprint CERN-EP-2000-008, CERN, 2000, submitted to Phys. Lett. B; "Search for supersymmetric particles in scenarios with a gravitino LSP and stau NLSP", Preprint CERN-EP-2000-015, CERN, 2000, submitted to E. Phys. J. C.
69. L3 Collab., M. Acciarri *et al*, Phys. Lett. **B 471** (1999) 280; Phys. Lett. **B 472** (1999) 420; Phys. Lett. **B 471** (1999) 308.
70. OPAL Collab., G. Abbiendi *et al*, "Search for Chargino and neutralino Production at $\sqrt{s}$ = 189 GeV at LEP", Preprint CERN-EP/99-123, CERN, 1999, submitted to E. Phys. J. C; "Photonic Events with Missing Energy in e^+e^- Collisions at $\sqrt{s} = 189$ GeV", Preprint CERN-EP-2000-060, CERN, 2000, submitted to E. Phys. J. C.
71. DELPHI Collab., P. Abreu *et al*, E. Phys. J. **C 11** (1999) 1.
72. L3 Collab., M. Acciarri *et al*, Phys. Lett. **B 482** (2000) 31.
73. CDF Collab., F. Abe *et al*, Phys. Rev. Lett. **81** (1998) 1791.
74. J.L. Lopez and D.V. Nanopoulos, Phys. Rev. **D 55** (1997) 4450.